Hybrid Spiral Superb Fairy-wren Optimization Algorithm for Economic Load Dispatch Problem

Xin-Yi Guan, Jie-Sheng Wang *, Hao-Ming Song, Jia-Hui Zhao

Abstract—**To address the limitations of the traditional Splendid Fairy-wren Optimization Algorithm (SFOA) in complex high-dimensional search spaces, namely, its susceptibility to local optima and its slow convergence speed, this paper proposes a novel Hybrid Spiral Splendid Fairy-wren Optimization Algorithm (HSSFOA). The proposed algorithm preserves the original three-phase behavioral model of chick growth, foraging, and predator evasion, while integrating the escape energy mechanism from the Harris Hawks Optimization (HHO) algorithm to enhance global exploration capabilities. Additionally, the spiral search strategy from the Whale Optimization Algorithm (WOA) is incorporated to improve local exploitation performance. To further enhance jump diversity and convergence efficiency, five distinct spiral update strategies are designed: sine spiral, phase-modulated spiral, hyperbolic sine spiral, hyperbolic cosine spiral, and damped spiral. To comprehensively evaluate the performance of the proposed algorithm, it is initially tested on 30 benchmark functions from the CEC-2017 suite to assess its performance in high-dimensional optimization tasks. Subsequently, the algorithm is applied to solve both a 6-unit and a 20-unit Economic Load Dispatch (ELD) problem in a power system. The results are compared with those from other state-of-the-art optimization algorithms. Experimental results demonstrate that HSSFOA significantly outperforms several contemporary algorithms in terms of convergence speed, solution quality, and robustness across different problem scales. These findings highlight the potential of HSSFOA as an efficient and scalable optimization framework for real-time economic dispatch in power systems.**

Index Terms—**Splendid Fairy-wren Optimization Algorithm, Hybrid Spiral Strategy, Escape Energy Mechanism, Spiral Search Strategy, Economic Load Dispatch**

I. Introduction

In contemporary engineering and scientific research, complex high-dimensional optimization problems pervade areas such as image processing, machine learning, network optimization, and energy scheduling. Economic Load Dispatch (ELD) in power systems represents a prototypical instance of a high-dimensional, tightly coupled, constrained non-convex optimization problem. Its objective is to minimize total generation cost while satisfying both power balance constraints and the individual output limits of each generating unit. With the increasing penetration of renewable energy sources and the growing complexity of electricity market transactions, the ELD problem exhibits pronounced multimodality, nonlinearity, non-convexity, and high-dimensional coupling. Classical gradient-based methods and Lagrange multiplier techniques often fail to procure global optimality or rapid convergence in large-scale, real-time dispatch settings, owing to cost-function discontinuities, forbidden operating zones, and valve-point effects [1].

In recent years, meta-heuristic algorithms based on swarm intelligence have garnered increasing attention due to their simplicity, few control parameters, and ability to conduct parallel exploration in large-scale search spaces. Algorithms such as Particle Swarm Optimization (PSO) [2], Differential Evolution (DE) [3] and Ant Colony Optimization (ACO) [4] have demonstrated remarkable performance in a variety of engineering applications. However, these algorithms often suffer from premature convergence and local optima entrapment when dealing with extremely complex and high-dimensional multi-modal landscapes, leading to an imbalance between global exploration and local exploitation.

To address the limitations associated with classical swarm intelligence algorithms, such as premature convergence and slow convergence speed, a variety of enhanced methods have been proposed. Fang et al. introduced the multi-strategy fusion dung beetle optimizer (MSFDBO), a novel approach that mitigates these issues by expanding the search space during the initial phase through refractive opposition-based learning. This strategy prevents premature convergence to local optima by incorporating an adaptive curve-based population control mechanism. Additionally, triangular drift strategies and fusion subtractive average optimizers were integrated into the rolling and mating behaviors of dung beetles, while an adaptive Gaussian-Cauchy hybrid perturbation factor was employed to significantly improve the overall performance of the algorithm [5]. In a similar vein, Wang et al. developed a reinforcement learning-enhanced differential evolution algorithm. This method integrates Q-learning into differential evolution (DE) to dynamically adjust algorithm parameters and select appropriate mutation strategies, thus improving both adaptability and overall optimization performance [6]. Xu et al. proposed an enhanced variant of the Honey Badger Algorithm (HBA) known as SHBA, which incorporates symbiotic mechanisms based on cooperative interactions between honey badgers and

Manuscript received May 8, 2025; revised July 10, 2025. This work was supported by the Basic Scientific Research Project of Institution of Higher Learning of Liaoning Province (Grant No. LJ222410146054), and Postgraduate Education Reform Project of Liaoning Province (Grant No. LNYJG2022137).

Xin-Yi Guan is a postgraduate student at School of Electronic and Information Engineering, University of Science and Technology Liaoning, Anshan, 114051, P. R. China (e-mail: gxy@stu.ustl.edu.cn).

Jie-Sheng Wang is a professor of School of Electronic and Information Engineering, University of Science and Technology Liaoning, Anshan, 114051, P. R. China (Corresponding author, phone: 86-0412-2538246; fax: 86-0412-2538244; e-mail: wjs@ustl.edu.cn).

Hao-Ming Song is a doctoral student of School of Electronic and Information Engineering, University of Science and Technology Liaoning, Anshan, 114051, P. R. China (e-mail: shm@stu.ustl.edu.cn).

Jia-Hui Zhao is a postgraduate student at School of Electronic and Information Engineering, University of Science and Technology Liaoning, Anshan, 114051, P. R. China (e-mail: zjh@stu.ustl.edu.cn).

honey guided birds. This symbiosis enhances population diversity while maintaining the search capability of the algorithm. Their approach demonstrated strong competitive performance in experimental settings [7]. Chaib et al. introduced an innovative hybridization of the Crayfish Optimization Algorithm (COA) with a fractional-order chaotic map. This hybrid model includes an adaptive COA parameter setting and a dimensional learning-hunting search scheme, leading to improvements in accuracy, consistency, and convergence speed [8]. Similarly, Jia et al. enhanced the COA by embedding a water-quality-based environmental update mechanism and a ghost-antagonistic learning strategy, which significantly bolstered the algorithm's ability to escape local optima and enhance global search performance [9]. In the context of marine ecosystem modeling, Ye et al. introduced an adaptive weight adjustment strategy and a dynamic social learning mechanism into the Marine Predators Algorithm (MPA). These innovations markedly increased encounter rates and improved search efficiency, which are essential for optimizing search strategies in complex environments [10]. Qian et al. enhanced the Chimpanzee Optimization Algorithm (ChOA) by combining it with six spiral functions, yielding results that were highly competitive compared to traditional methods, further validating the algorithm's robustness [11]. Lastly, Huang et al. addressed the shortcomings of the Aurora Optimization Algorithm in terms of both population diversity and convergence speed by introducing a pseudo-random lens SPM chaotic initialization strategy. They further proposed a hybrid approach combining adaptive dynamics with a locally exploitative reward-loss function and incorporated an adaptive t-distribution mutation mechanism. These improvements significantly enhanced both population diversity and the convergence speed of the algorithm [12]. Together, these advancements reflect the ongoing efforts to refine swarm intelligence algorithms, making them more adaptable, efficient, and capable of overcoming the inherent limitations of classical approaches.

The Superb Fairy-wren Optimization Algorithm (SFOA) [13] simulates the behavioral processes of chick development, foraging, and predator evasion across three stages, exhibiting good adaptability in solving multi-modal functions. By dynamically adjusting search strategies through stage-wise behavioral modeling, the algorithm enhances population diversity during exploration. However, as the problem dimensional and complexity increase, the original SFOA reveals limitations in both global search efficiency and local exploitation accuracy. Specifically, it tends to fall into local optima in high-dimensional spaces and suffers from limited convergence speed due to constraints inherent in its behavior-driven search mechanisms.

To address these limitations, this paper proposes a Hybrid Spiral Multistage Superb Fairy-wren Optimization Algorithm (HSSFOA). Building upon the original three-phase behavioral model, the proposed algorithm incorporates the escape energy mechanism of the Harris Hawks Optimization (HHO) algorithm [14] to enhance global exploration capability. Simultaneously, it integrates the spiral search strategy of the Whale Optimization Algorithm (WOA) [15] to strengthen local search performance. Moreover, to investigate the influence of movement trajectories on jump diversity and convergence efficiency, five spiral update strategies are introduced: sine spiral, phase-modulated spiral, hyperbolic sine spiral, hyperbolic cosine spiral, and damped spiral. This design aims to achieve a more effective balance between global exploration and local exploitation. Subsequently, HSSFOA will be comprehensively evaluated on the high-dimensional benchmark suite CEC-BC-2017 [16], followed by comparative experiments on a 6-unit and a 20-unit economic load dispatch (ELD) system to assess its practical performance [17]. The experiments will systematically investigate the algorithm's convergence behavior, solution quality, and computational scalability, in comparison with several state-of-the-art methods. The results are expected to demonstrate that HSSFOA offers an efficient and scalable optimization framework for real-time economic dispatch in power systems.

II. Superb Fairy-wren Optimization Algorithm

A. Initialization

The proposed SFOA is a population-based technique that simulates its search capability in the solution space by varying the number of fitness evaluations, thereby effectively addressing the optimization problems in real-world environments. Each member of the SFOA represents a candidate solution to the problem and determines the values of decision variables based on the problem landscape within the search space. Mathematically, each member is modeled as a vector, where each element corresponds to a decision variable. The collection of all members constitutes the population of the algorithm, as defined in Eq. (1). Simultaneously, the initial positions of all members are initialized at the beginning of the algorithm by using Eq. (2).

$$X = \begin{bmatrix} X_1 \\ \vdots \\ X_i \\ \vdots \\ X_N \end{bmatrix}_{N\times D} = \begin{bmatrix} X_{1,1} & \cdots & X_{1,d} & \cdots & X_{1,D} \\ \vdots & \ddots & \vdots & \ddots & \vdots \\ X_{i,1} & \cdots & X_{i,d} & \cdots & X_{i,D} \\ \vdots & \ddots & \vdots & \ddots & \vdots \\ X_{N,1} & \cdots & X_{N,d} & \cdots & X_{N,D} \end{bmatrix}_{N\times D} \quad (1)$$

$$X = (ub - lb) \times rand(0,1) + lb \quad (2)$$

where, X denotes the global population matrix of the SFOA, X_i represents the i-th member (candidate solution), and $X_{i,D}$ refers to the value of the d-th decision variable in the search space. N is the total number of population members, r is a uniformly distributed random number in the interval [0,1], and ub and lb denote the upper and lower bounds of the d-th decision variable, respectively.

B. Mathematical Model of the SFOA

In each evaluation, the positions of the SFOA population members are updated through three distinct phases: an initial global exploration inspired by chick growth behavior, followed by an exploitation phase based on foraging and mating activities, and finally a further exploitation phase driven by predator avoidance behavior.

1. Chick Growth Phase

The SFOA updates the position of each individual based on Eq. (3), aiming to improve the objective function value.

$$Xnew_{i,j} = X_{i,j}^t + (lb + (ub - lb) \times rand), r > 0.5 \quad (3)$$

where, $Xnew_{i,j}$ denotes the updated position of the population member, $X_{i,j}^{t}$ represents the position of the i-th member in the j-th dimension after t iterations, and $rand$ is a random number in the interval [0,1].

2. Reproduction and Foraging Phase

In this stage, the positions of all agents are revised by emulating the Splendid Fairy-wren's breeding and chick-rearing behaviors. When the risk threshold s, defined in Eq. (4), falls below a preset limit, the algorithm enters the breeding phase and enacts a specialized incubation barrier to prevent intrusion by foreign individuals.

$$s = r_1 * 20 + r_2 * 20 \tag{4}$$

where, r_1 and r_2 are random numbers drawn from a normal distribution. Due to the cooperative breeding behavior of the SFOA, multiple members incubate eggs year-round, promoting recognition and learning. During each cycle (m), SFOA members alternate between foraging and teaching, leading to small positional adjustments that enhance the efficiency of local search exploitation. A maturity factor is introduced, which increases as the teaching cycle progresses. As members approach the maturity phase, their activity range expands. Based on the modeling of positional changes during teaching and egg incubation, each member's new position is computed by using Eq. (5). If this new position results in an improved objective function value, the corresponding member is updated.

$$Xnew_{i,j} = X_G + (X_b - X_{i,j}^{t}) \times p\ , r < 0.5\ and\ s < 20 \tag{5}$$

$$X_G = X_b \times C \tag{6}$$

where, X_b denotes the current best position, and C is a constant with a value of 0.8.

$$p = sin((ub - lb) \times 2 + (ub - lb) \times m) \tag{7}$$

$$m = \left(\frac{FEs}{MaxFEs}\right) \times 2 \tag{8}$$

where, FEs denotes the current number of iterations, and $MaxFEs$ represents the maximum number of iterations.

3. Predator Avoidance Phase

In the predator avoidance phase of the SFOA, the positions of the population members are updated based on the defense mechanisms employed by the Splendid Fairy-wren against predators. Its movement pattern is described by the mathematical formula in Eq. (9).

$$Xnew_{i,j} = X_b + X_{i,j} \times l \times k\ , r < 0.5\ and\ s > 20 \tag{9}$$

where, l represents the Levy flight random step size, which controls the algorithm's ability to escape from local optima. k is the adaptive flight balance factor, as described in Eq. (10), and works in conjunction withlto adjust the flight distance of the birds. Additionally, X_b is incorporated to control the movement direction of the birds.

In this formulation, W denotes the call frequency, which plays a critical role in facilitating predator avoidance by acting as an early alert signal during flight.

$$k = 0.2 \times sin\left(\frac{\pi}{2} - w\right) \tag{10}$$

$$w = \frac{\pi}{2} \times \frac{FEs}{MaxFEs} \tag{11}$$

III. Hybrid Spiral Superb Fairy-wren Optimization Algorithm

A. Hybrid Superb Fairy-wren Optimization Algorithm

To address the issues of local optima and slow convergence speed in the Splendid Fairy-wren Optimization Algorithm (SFOA), we propose a Hybrid Spiral SFOA. Given that the Harris Hawks Optimization (HHO) [14] algorithm has strong global search capabilities, and the spiral search mechanism in the Whale Optimization Algorithm (WOA) [15] enables both broad global exploration and fine local development, we integrate these two algorithms into the SFOA to enhance its search ability and help it escape local optima. Specifically, the original position update Eq. (5) is replaced with position updates derived from both algorithms. To balance the contributions of the two algorithms, we introduce the escape energy formula from HHO shown in Eq. (12) to determine which update strategy to apply.

When the escape energy $|E0| >= 1$, the random leap update from HHO is used (Eq. (13)); when $|E0| < 1$, the spiral search update from WOA is employed (Eq. (14)). Through this adaptive switching mechanism based on escape energy, the algorithm efficiently explores the global search space and refines solutions locally near the optimal solution, significantly enhancing its ability to escape from local optima and accelerating its overall convergence speed.

$$E = (2 \times rand - 1) \times 2 \times \left(1 - \frac{FEs}{MaxFEs}\right) \tag{12}$$

$$Xnew_{i,j} = X_{i,j} - rand \times \left|(2 \times rand - 1) \times X_b - X_{i,j}\right| \tag{13}$$

$$Xnew_{i,j} = \left|X_b - X_{i,j}\right| \times Z + X_b \tag{14}$$

$$Z = e^{b+r} \times cos(2\pi r) \tag{15}$$

$$r = \left(-2 - \frac{FEs}{MaxFEs}\right) \times rand + 1 \tag{16}$$

where, Z represents spiral in WOA, and b is set to 1.

B. Hybrid Spiral Superb Fairy-wren Optimization Algorithm

To further enrich the diversity and adaptability of the search trajectories, this paper introduces five spiral shapes with distinct geometric characteristics, based on the original spiral update formula of the Whale Optimization Algorithm (WOA). These spirals are designed to guide the algorithm's jumping path during different iterative stages. They include: sine spiral, phase-modulated logarithmic spiral, hyperbolic sine spiral, hyperbolic cosine spiral, and damping spiral. The original WOA spiral is shown in Fig. 1(a), while the other five spirals are depicted in Fig. 1(b)-(f). Their mathematical expressions are provided in Table I. By randomly or strategically switching among these spiral shapes during each spiral update, the algorithm can obtain more diverse search paths during the local exploitation phase, thus enhancing its ability to escape local optima and accelerating overall convergence. Furthermore, this dynamic shape switching mechanism can effectively balance the exploration and development capabilities of the algorithm. When the algorithm detects search stagnation, it enhances global exploration by switching to a high-curvature helix. In the stable convergence stage, progressive helical enhancement for local refinement is adopted to further optimize the coverage efficiency of the search space.

TABLE I. THE FORMULA OF FIVE KINDS OF SPIRALS

Serial number	Screw name	Formula	Parameter setting
1	Sine spiral	$e^{b+r} \times (1 + a \times sin(c \times 2\pi r))$	a=0.3; b=1; c=5
2	Phase modulation Log spiral	$e^{b+r} \times (1 + a \times sin(c \times 2\pi r + h)) \times cos(2\pi r)$	a=0.3; b=1; c=6; h=π/4
3	Sinh spiral	$\sinh(\mathrm{a} \times 2\pi r) \times cos(2\pi r)$	a=0.5
4	Cosh spiral	$\cosh(\mathrm{a} \times 2\pi r) \times cos(2\pi r)$	a=0.5
5	Damping spiral	$e^{-a \times 2\pi r} \times 2\pi r \times cos(2\pi r)$	a=0.2

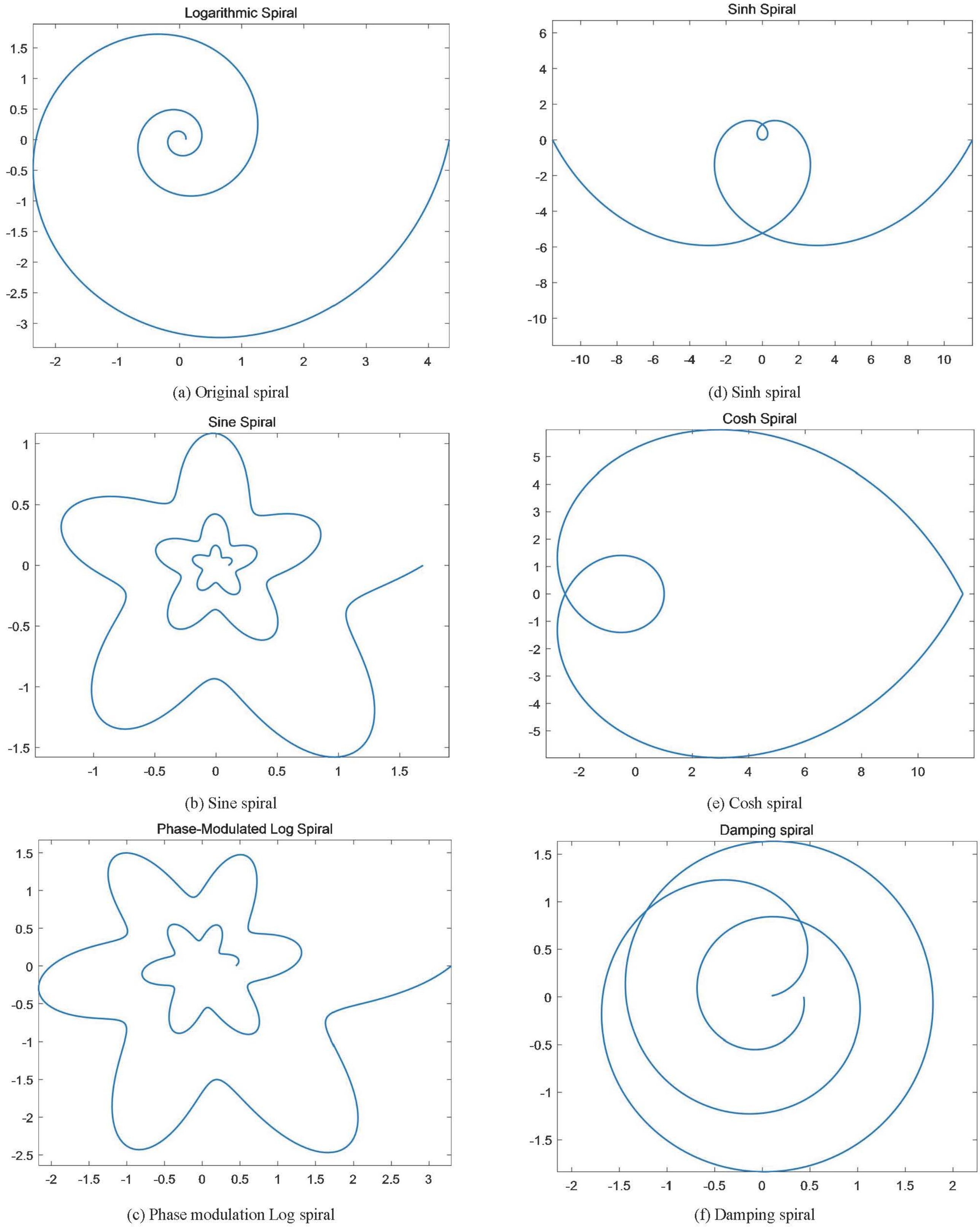

(a) Original spiral

(d) Sinh spiral

(b) Sine spiral

(e) Cosh spiral

(c) Phase modulation Log spiral

(f) Damping spiral

Fig. 1 Images of the spirals.

C. Pseudo-code and Flowchart of the HSSFOA

Pseudo code of HSSFOA:

```
Initialize the parameters and population
Calculate the fitness of the initialized population and find the best individual (FEs=FEs+1)
WHILE(FEs<=MaxFEs)
  FOR i=1 to N
    IF r>T (Young birds make up a large proportion of population)
      Entering the growth stage of young birds, the position update was carried out according
       to Eq. (3). (Young birds growth stage)
    ELSE
      Calculate the danger factor s of the current position according to Eq. (4).
        IF s<R (The current environment is safe)
            IF |E0|>=1 The position is updated by Eq. (13). (Random jump of HHO)
            ELSE The position is updated by Eq. (14). (Spiral search of WOA)
            END IF
        ELSE (The current environment is dangerous)
          The natural enemies were avoided by Eq. (9). (Avoiding natural enemies stage)
        END IF
     END IF
  END FOR
END WHILE
Calculate the fitness of the updated population and find the best individual (FEs=FEs+1)
END
```

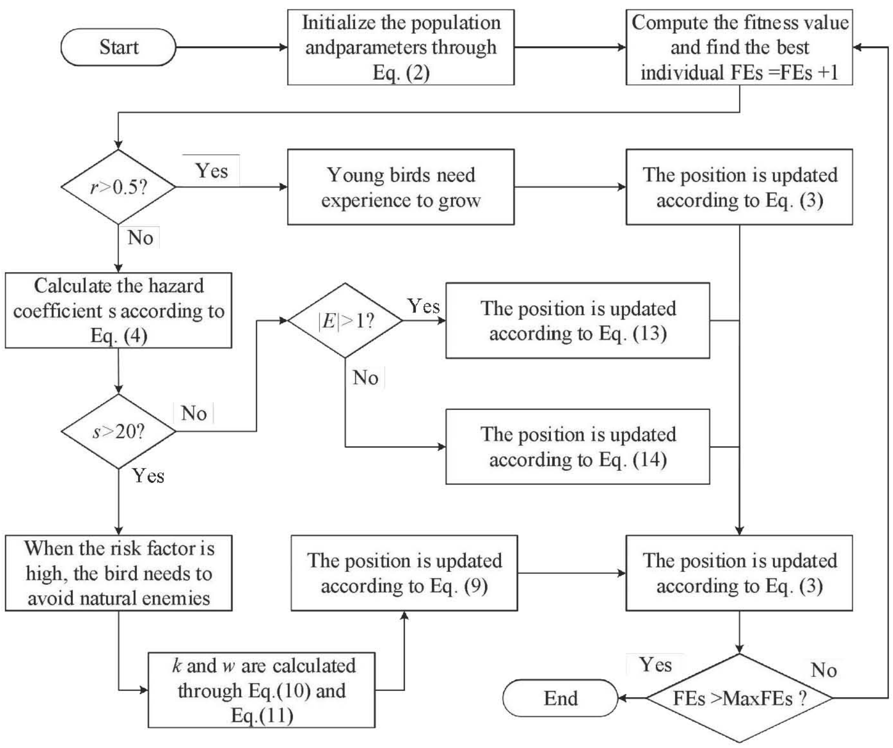

Fig. 2 The flow chart of HSSFOA.

IV. SIMULATION EXPERIMENT AND ANALYSIS

To comprehensively evaluate the optimization performance and practical applicability of the proposed Hybrid Spiral Super-Flock Optimization Algorithm (HSSFOA), three representative groups of experiments were designed and conducted, targeting both standard benchmark functions and real-world engineering problems. The experiments aim to systematically analyze the performance of HSSFOA in solving complex optimization tasks characterized by high dimensionality, multimodality and nonlinearity, while examining its global search capability, local exploitation ability, and overall robustness. Furthermore, the impact of different spiral-guided strategies on the algorithm's search behavior and optimization outcomes is also investigated.

The first set of experiments employed the 30 benchmark functions from the CEC-BC-2017 test suite, which include unimodal, multimodal, separable, non-separable and rotated functions, thereby covering a wide range of optimization characteristics. This evaluation comprehensively assesses the adaptability and stability of HSSFOA in standard optimization environments. Comparative experiments were conducted against various classical and recently developed intelligent optimization algorithms. Performance metrics such as best value, mean value, standard deviation, and convergence curves were used to verify the proposed algorithm's superiority in terms of solution accuracy, convergence speed, and stability.

The second set of experiments focuses on real-world engineering optimization scenarios, where the proposed HSSFOA is applied to economic load dispatch (ELD) problems in power systems. Two case studies with different scales are conducted to thoroughly evaluate the algorithm's practical applicability.

In the first case, a classical 6-unit power system is considered, where the objective is to meet a total load demand of 1263 MW while minimizing the total fuel cost. This problem includes generation limits and transmission losses, posing a moderately complex yet widely recognized benchmark for testing algorithmic performance. HSSFOA's performance on this system is evaluated in terms of cost minimization, convergence behavior, and constraint handling capabilities, and compared with several well-known optimization algorithms.

In the second case, a large-scale 20-unit system is used, where the goal is to schedule generation to satisfy a total demand of 2500 MW. This problem is characterized by high nonlinearity, a vast solution space, and complex operational constraints, making it a more challenging tested for scalability and robustness. In this scenario, HSSFOA aims to minimize the total operational cost while strictly satisfying all system constraints. The performance is assessed using metrics such as total generation cost, convergence speed, and solution stability, and benchmarked against both classical and modern meta-heuristic algorithms.

These two complementary case studies provide a comprehensive evaluation of HSSFOA's effectiveness across small- and large-scale constrained engineering optimization problems.

A. HSSFOA Solves CEC-BC-2017 Benchmark Functions

To thoroughly evaluate the effectiveness and optimization performance of the proposed Hybrid Spiral Superb Fairy-wren Optimization Algorithm (HSSFOA), this study conducted a systematic experimental assessment based on the CEC-BC-2017 benchmark suite. This suite includes 30 representative, complex, high-dimensional benchmark functions, encompassing single-modal, multi-modal, composite functions, and high-dimensional coupling problems, which effectively test the adaptability of optimization algorithms across different problem structures. All test functions were set to a dimension of 30, with variable ranges defined as [-100,100], a maximum iteration count of 1000, and a population size of 30, ensuring a fair evaluation of the algorithm in a standardized environment. To guarantee the reliability and statistical significance of the experimental results, each experimental set was independently run 30 times, and performance analysis was conducted based on three metrics: Mean, Best, and Standard Deviation (Std).

To compare the specific impacts of different strategies on the algorithm's performance, the improved SFOA algorithm was named ISFOA, and five variants were constructed based on five different types of spiral trajectory update strategies: SISFOA with sine spiral mechanism, LISFOA incorporating phase-modulated logarithmic spiral, SHISFOA with hyperbolic sine spiral, CHISFOA with hyperbolic cosine spiral, and DISFOA with damping spiral strategy. These improvements aimed to enhance the population's jumping diversity and local development capability, thereby improving overall optimization efficiency. The convergence curve of the experimental results is shown in Fig. 3, and the statistical table of the experimental results is shown in Table II. In addition, according to the average value of the experimental results in Table II, we draw an inward circular histogram, as shown in Fig. 4, the closer to the center of the circle, the better the effect of the algorithm.

According to the convergence curves and histograms of Fig. 3 and Fig. 4, HSSFOA and its variants show faster convergence speed and higher stability on multiple functions. Notably, they demonstrate strong global exploration capability in the early search phase, with the convergence stabilizing in the later stages, thus avoiding premature convergence to local optima. As shown in the detailed statistical results in Table II, compared to the original SFOA algorithm, the improved algorithms achieved significant improvements on most test functions. The experimental results reveal the performance of each algorithm variant across different test functions. In the case of the F1 function, ISFOA achieved the best results, attaining near-optimal mean and standard deviation values, significantly outperforming the original SFOA. SISFOA also performed well, ranking second, showcasing its strong global search capability. For the F2 function, DISFOA demonstrated superior performance, with its damping mechanism stabilizing the late-stage search and preventing premature convergence. SISFOA also showed good results, leveraging its jump search mechanism to avoid premature trapping in local optima. In the F3 function, DISFOA achieved the best optimization results, particularly in terms of convergence speed and stability, while ISFOA and SISFOA also demonstrated robustness in tackling the function's complexity. For F4, LISFOA performed notably well, benefiting from its phase-modulation strategy, which proved effective for handling complex function structures. SISFOA followed closely behind, demonstrating its ability to balance global exploration with local refinement. On F5, ISFOA obtained the optimal optimization results, improving both the accuracy and standard deviation. SISFOA again showed its global search strengths, ranking second. In the F6 function, LISFOA took the lead, owing to its phase-modulation strategy, which proved advantageous in complex function structures, while SISFOA and DISFOA also performed well, maintaining stability during the search. For the F7 function, ISFOA exhibited superior performance, avoiding early convergence and demonstrating strong global exploration capabilities. SISFOA also achieved near-optimal results, ranking second. On F8, DISFOA stood out, as its damping mechanism effectively stabilized the late-stage search, outperforming other algorithms. In the case of the F9 function, SISFOA led the performance, owing to its spiral search mechanism, which excelled in high-dimensional jump searches. ISFOA ranked second, highlighting its robustness in global search scenarios. In the F10 function, ISFOA outperformed the other algorithms, reaching the best optimization results and minimizing the standard deviation. SISFOA and LISFOA also demonstrated robust performance, confirming their effective search strategies. For F11, LISFOA excelled, showcasing its phase-modulation strategy's advantages in complex high-dimensional functions, with SISFOA and ISFOA performing consistently well. On F12, SISFOA achieved the best optimization result, significantly improving both the accuracy and standard deviation. LISFOA followed closely behind, confirming the robustness of phase modulation in handling complex structures. For the F13 function, CHISFOA and SHISFOA led the results, demonstrating the advantages of hyperbolic functions in controlling convergence within local search regions. ISFOA and SISFOA also performed well, confirming their capability in multi-modal optimization tasks. In F14, CHISFOA and SHISFOA again showcased their strengths, with hyperbolic functions effectively guiding the algorithm to better convergence. For F15, LISFOA performed the best, benefiting from its phase-modulation strategy in addressing complex function structures, while SISFOA and ISFOA followed with stable results. In F16, LISFOA achieved the best results, reflecting its adaptability in complex, high-dimensional optimization spaces. SISFOA and ISFOA continued to display strong performance. On F17, LISFOA once again demonstrated the best performance, confirming its ability to handle complex functions effectively. SISFOA and ISFOA ranked well, showing consistent global search capability. For F18, ISFOA and SISFOA showed the best results, highlighting their superior global exploration capabilities. In the F19 function, ISFOA led the performance, showcasing its robustness in handling multi-peak functions, with SISFOA ranking second, further validating the efficacy of the spiral search mechanism. For F20, CHISFOA and SHISFOA exhibited the strongest performance, with hyperbolic functions ensuring effective convergence control in local regions. In F21, CHISFOA and SHISFOA again led, emphasizing the importance of hyperbolic functions for local search control, with ISFOA and SISFOA performing reliably. In F22, ISFOA achieved the best optimization results, particularly in terms of minimizing standard deviation. SISFOA and LISFOA demonstrated similar effectiveness, ensuring strong performance. For F23, CHISFOA and SHISFOA performed best, once again confirming the advantages of hyperbolic functions in local convergence. On F24, DISFOA emerged as the top performer, with its damping mechanism proving effective in stabilizing late-stage searches. For F25, CHISFOA and SHISFOA again led, showcasing their local convergence advantages, while SISFOA performed consistently well. In F26, ISFOA and SISFOA displayed the best results, highlighting their strong global search abilities. In F27, DISFOA took the lead, with its damping mechanism stabilizing the search and improving late-stage optimization. For F28, SISFOA achieved the best results, demonstrating superior performance in terms of both accuracy and standard deviation. In F29, LISFOA emerged as the best performer, benefiting from its phase-modulation strategy to handle complex function structures effectively. Finally, for F30, LISFOA again showed superior performance, demonstrating the advantages of its phase-modulation strategy in handling high-dimensional optimization problems. In conclusion, SISFOA, ISFOA, LISFOA, and other variants consistently demonstrated improved performance across the majority of the test functions. Overall, SISFOA and ISFOA exhibited the best overall optimization results, validating the effectiveness of the spiral mechanisms and multi-strategy collaborative updates in enhancing both global search capability and local refinement accuracy.

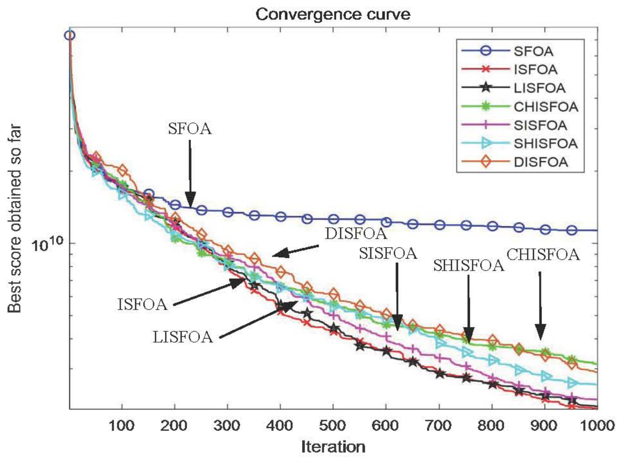

(1) f_1

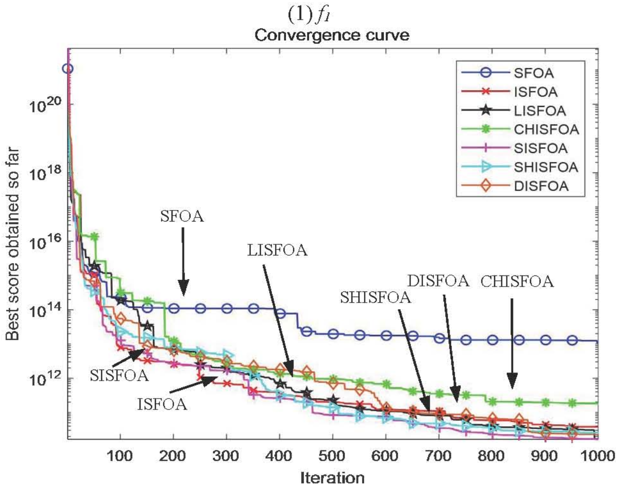

(2) f_2

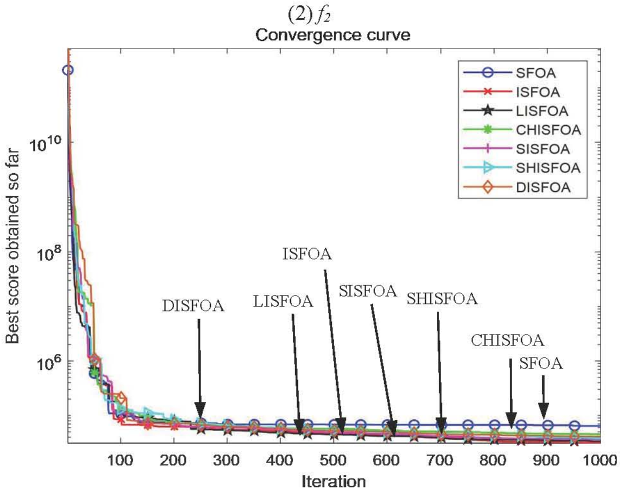

(3) f_3

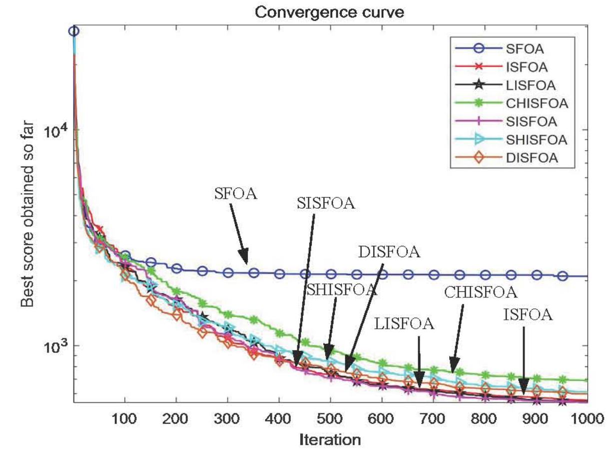

(4) f_4

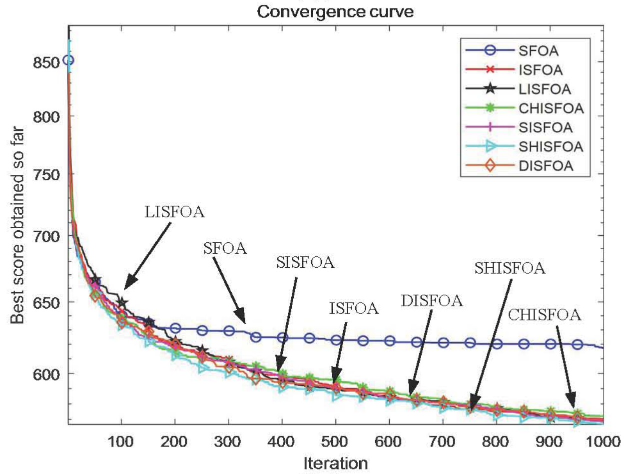

(5) f_5

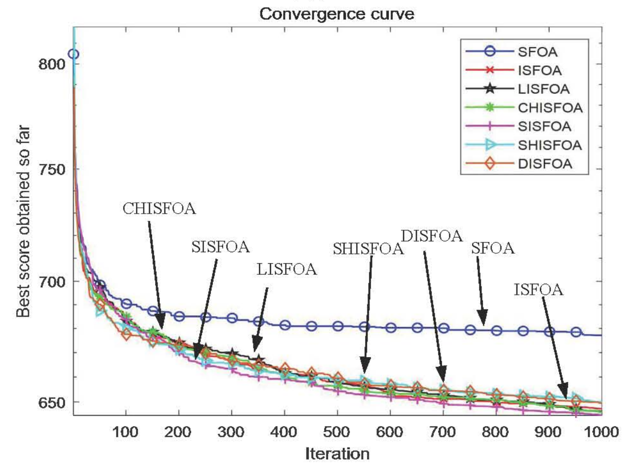

(6) f_6

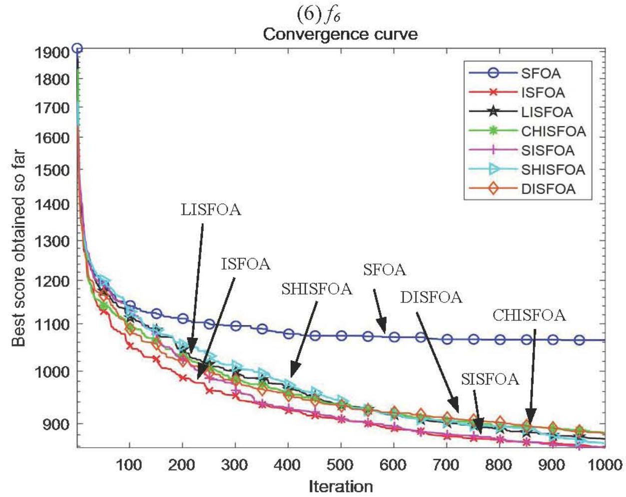

(7) f_7

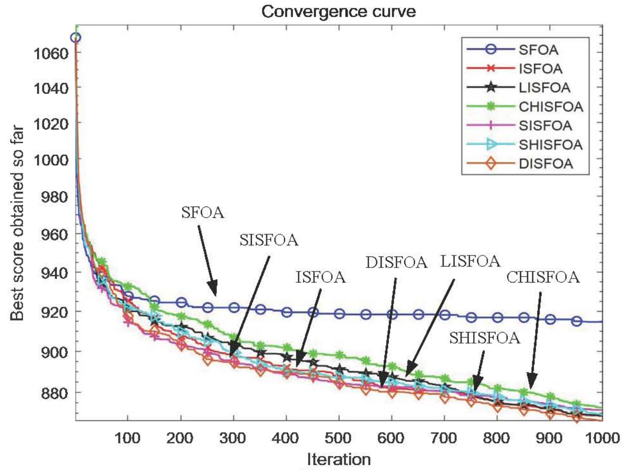

(8) f_8

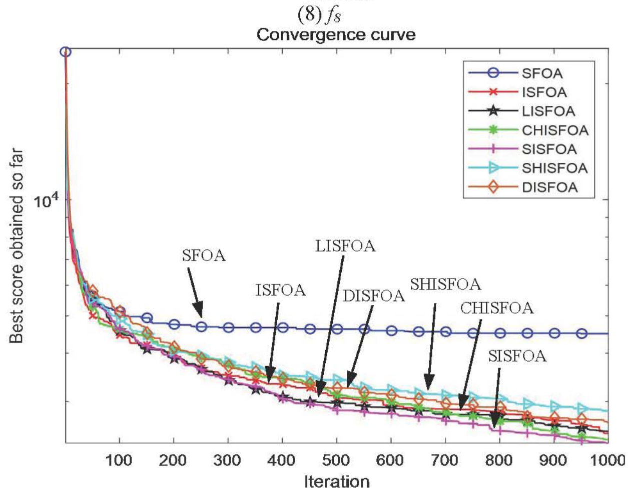

(9) f_9

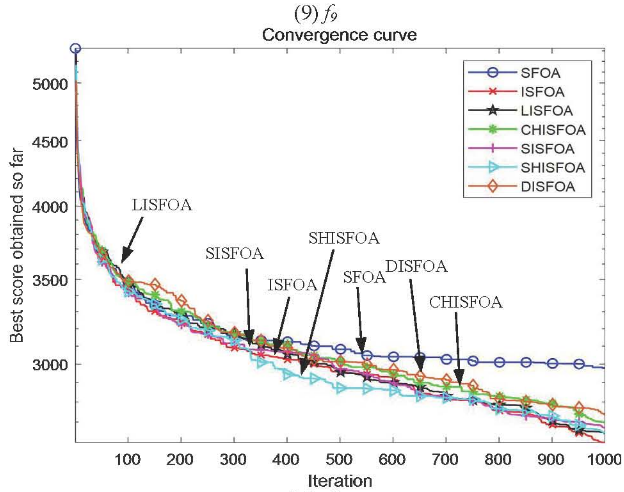

(10) f_{10}

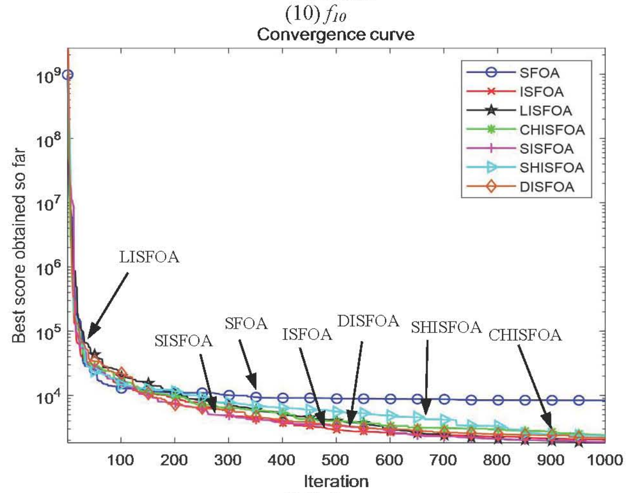

(11) f_{11}

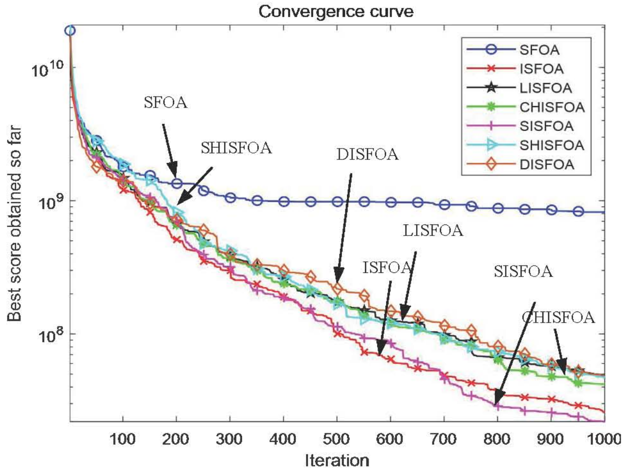

(12) f_{12}

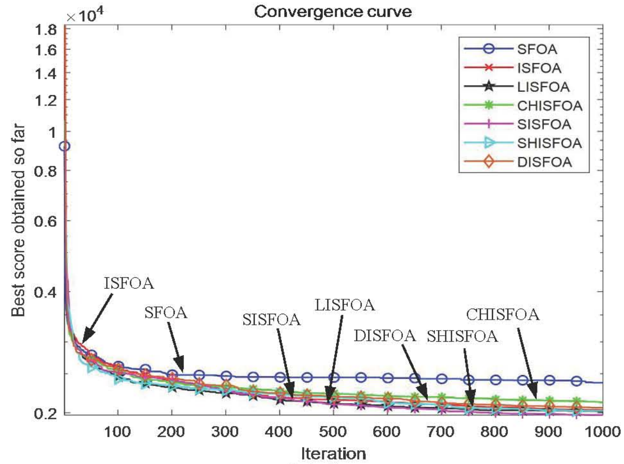

(16) f_{16}

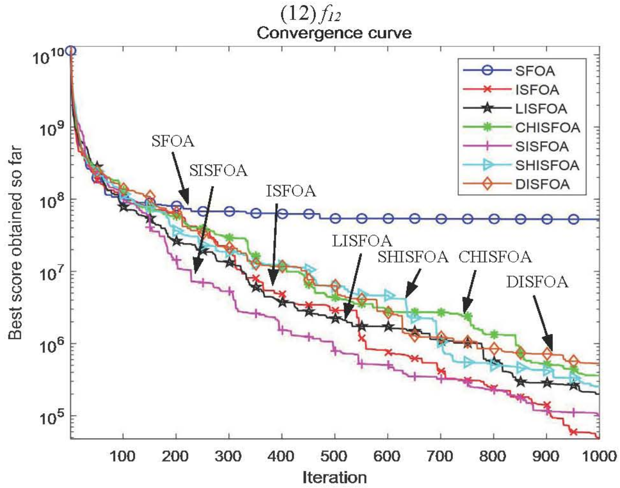

(13) f_{13}

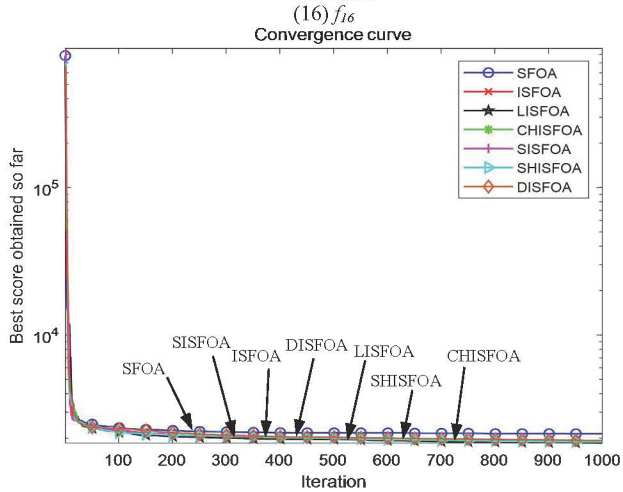

(17) f_{17}

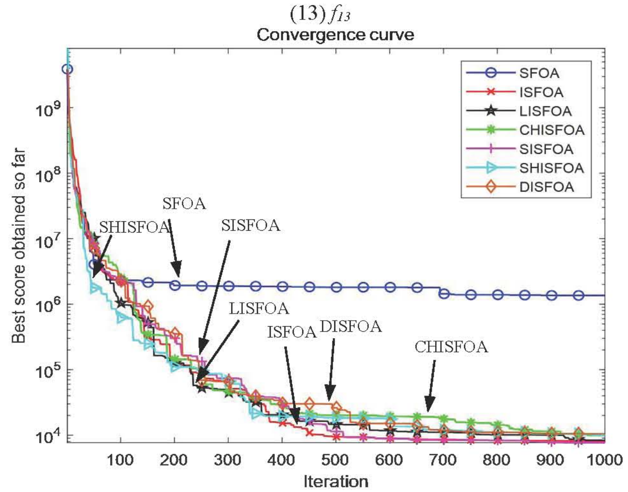

(14) f_{14}

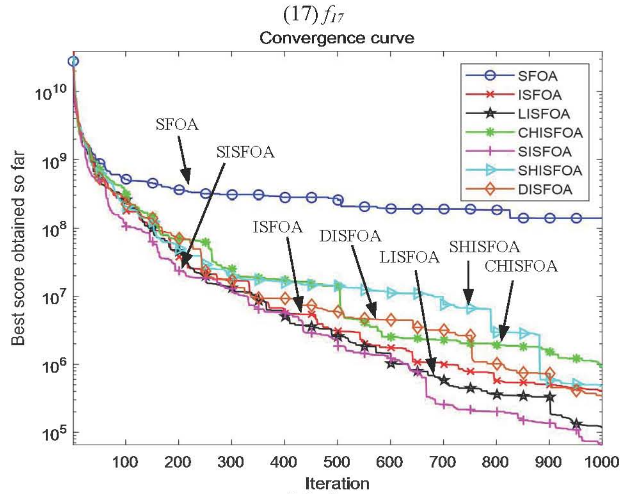

(18) f_{18}

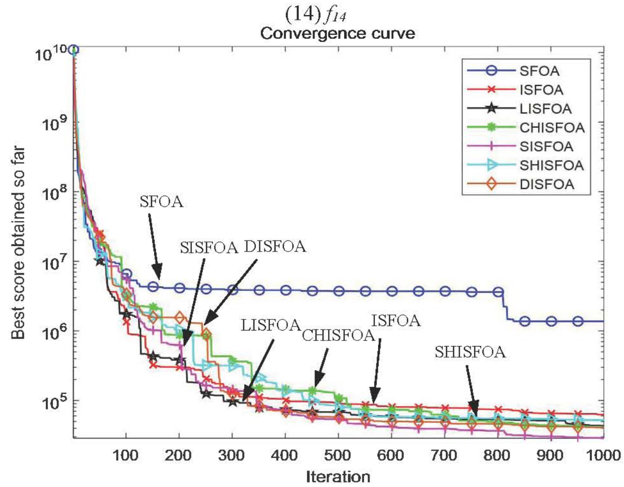

(15) f_{15}

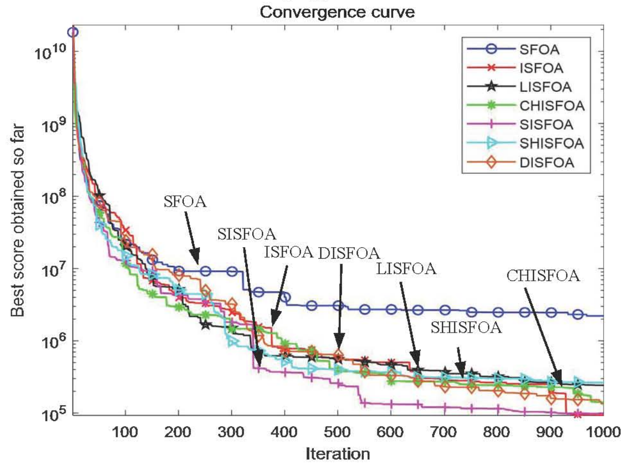

(19) f_{19}

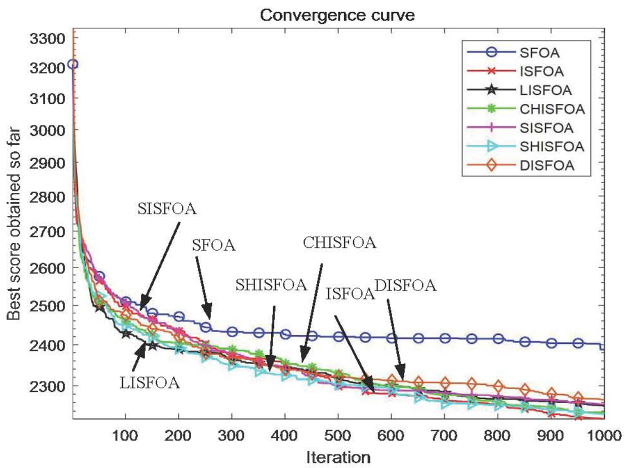

(20) f_{20}

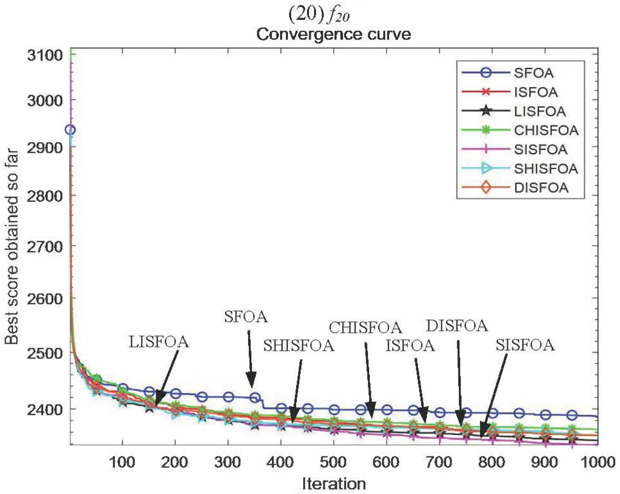

(21) f_{21}

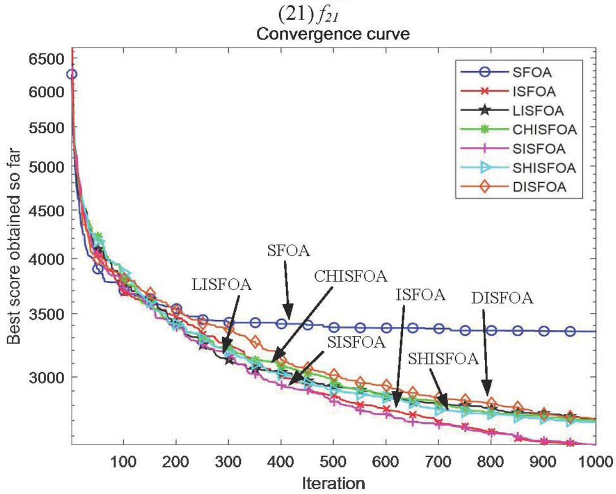

(22) f_{22}

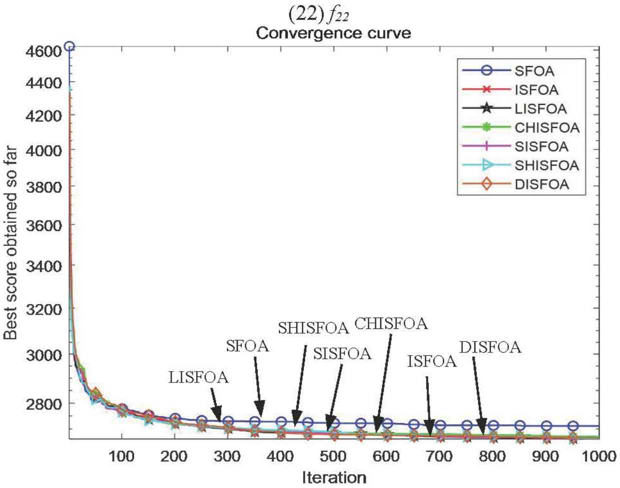

(23) f_{23}

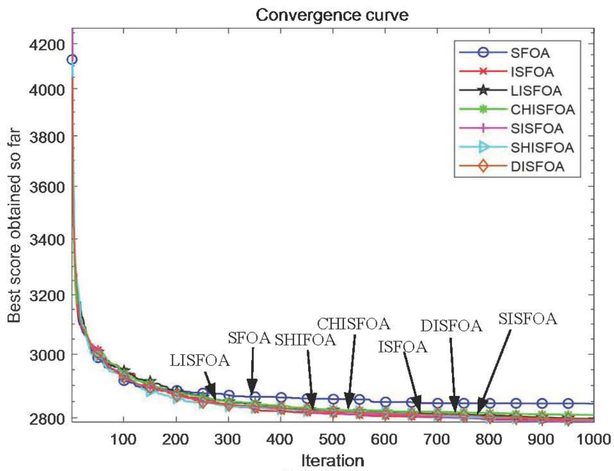

(24) f_{24}

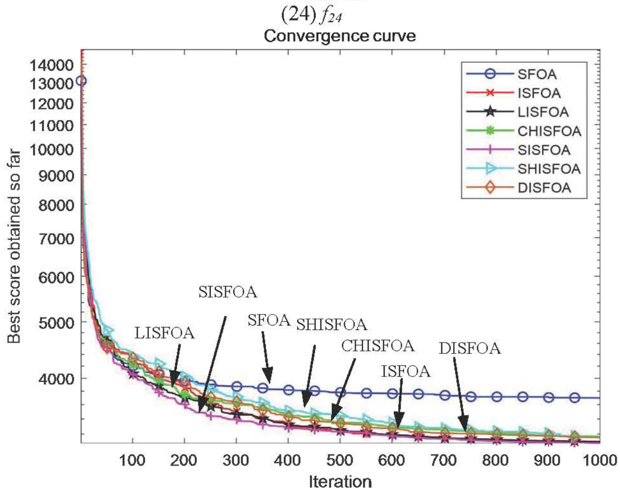

(25) f_{25}

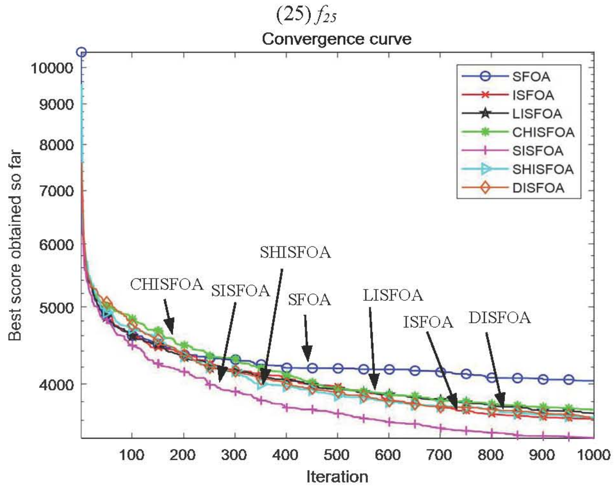

(26) f_{26}

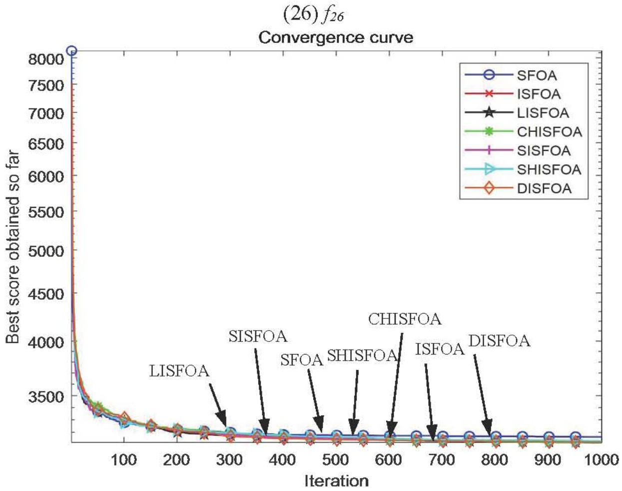

(27) f_{27}

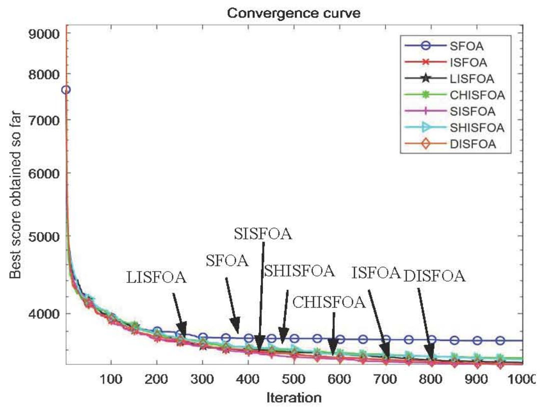

(28) f_{28}

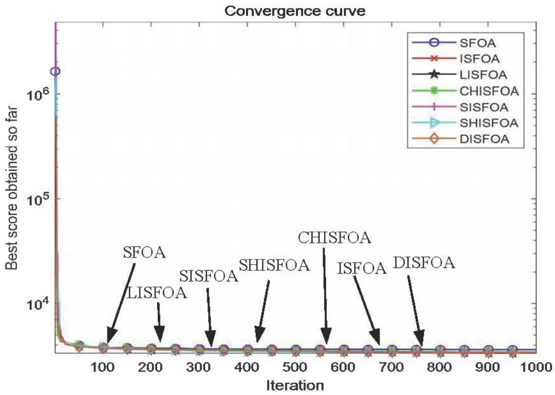

(29) f_{29}

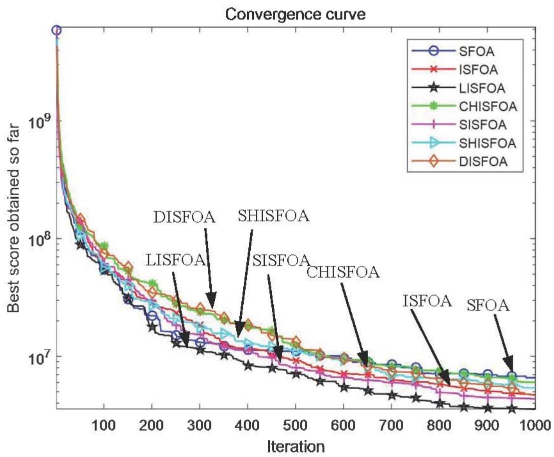

(30) f_{30}

Fig. 3 The convergence curves of HSSFOA to solve the CEC-2017 functions.

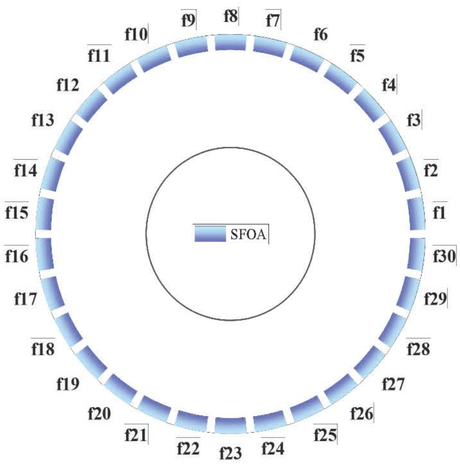

(a) SFOA

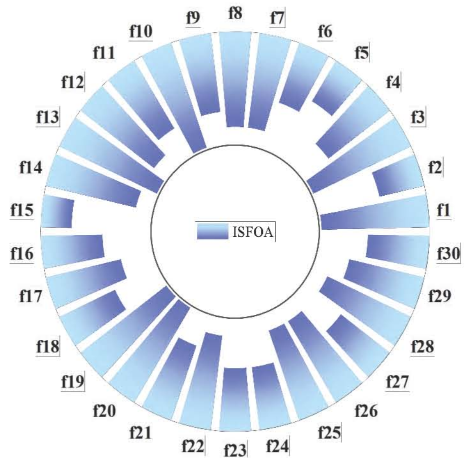

(b) ISFOA

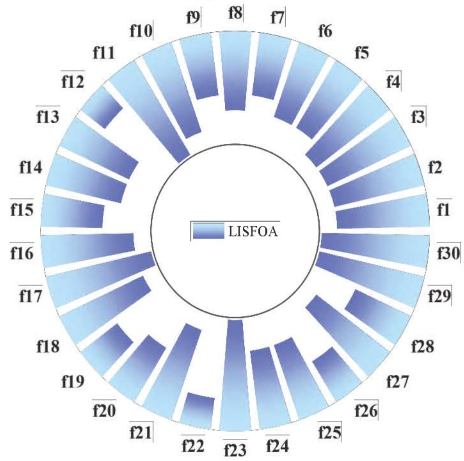

(c) LISFOA

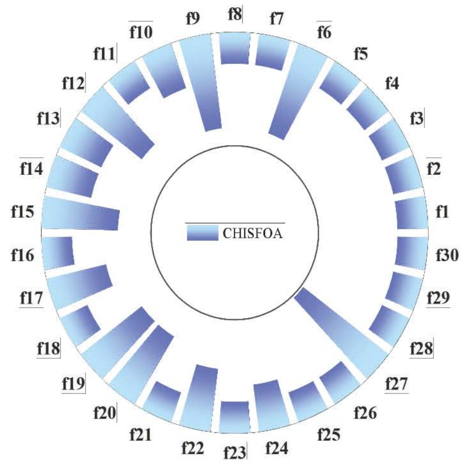

(d) CHISFOA

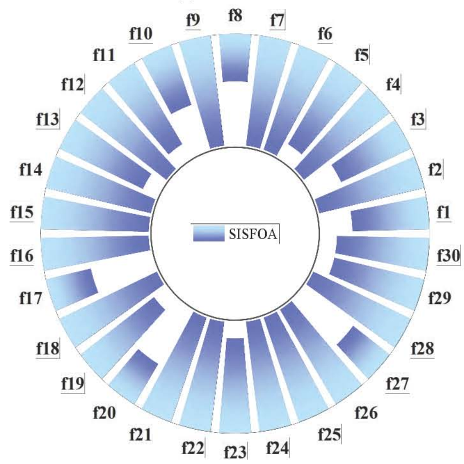

(e) SISFOA

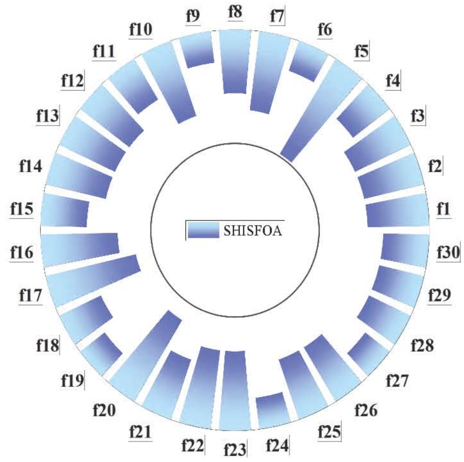

(f) SHISFOA

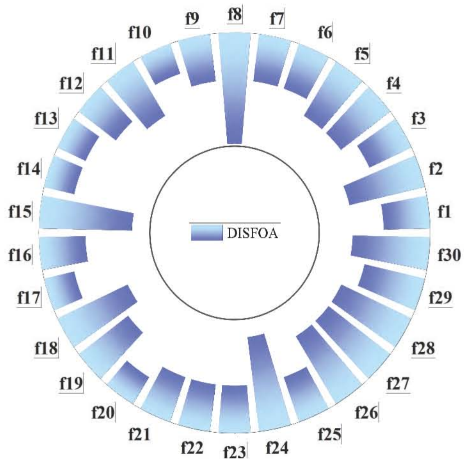

(g) DISFOA

Fig. 4 HSSFOA processes histograms of CEC-2017 test functions.

TABLE II. HSSFOA TO OPTIMIZE THE CEC-BC-2017 FUNCTIONS

Function		SFOA	ISFOA	LISFOA	CHISFOA	SISFOA	SHISFOA	DISFOA
f_1	Ave	1.1320E+10	**2.0364E+09**	2.0901E+09	3.1408E+09	2.2318E+09	2.5715E+09	2.9037E+09
	Std	5.5729E+09	1.4692E+09	1.6514E+09	2.3423E+09	**1.2804E+09**	1.9288E+09	2.2260E+09
	Best	3.5754E+09	2.2951E+08	3.0269E+08	2.8838E+08	3.9512E+08	**1.2019E+08**	7.4045E+08
	Rank	7	1	2	6	3	4	5
f_2	Ave	1.0958E+13	3.7667E+10	1.6866E+10	1.8347E+11	**1.6521E+10**	2.5598E+10	2.2188E+10
	Std	2.5253E+13	1.4469E+11	3.6474E+10	8.3091E+11	4.1213E+10	6.0282E+10	**3.3696E+10**
	Best	4.8211E+09	2.4098E+06	3.3245E+06	3.8277E+06	**2.5089E+05**	4.3395E+07	1.0973E+07
	Rank	7	5	2	6	1	4	3
f_3	Ave	6.4375E+04	**3.1264E+04**	3.3713E+04	4.4965E+04	3.6887E+04	3.8190E+04	4.0861E+04
	Std	3.1280E+04	**1.2853E+04**	1.5367E+04	2.0738E+04	1.3426E+04	1.7571E+04	1.5414E+04
	Best	1.4852E+04	1.0769E+04	1.2710E+04	1.3873E+04	9.4447E+03	9.9844E+03	**9.1027E+03**
	Rank	7	1	2	6	3	4	5
f_4	Ave	2.0953E+03	5.5923E+02	5.5118E+02	6.8416E+02	**5.4593E+02**	6.1137E+02	5.9858E+02
	Std	1.3192E+03	1.0423E+02	**8.7981E+01**	1.9881E+02	9.7194E+01	1.2203E+02	1.3572E+02
	Best	6.1054E+02	4.4756E+02	4.4228E+02	4.6615E+02	4.3017E+02	4.4212E+02	**4.1357E+02**
	Rank	7	3	2	6	1	5	4
f_5	Ave	6.1730E+02	5.7037E+02	5.6893E+02	5.7205E+02	5.6853E+02	**5.6689E+02**	5.6951E+02
	Std	2.6457E+01	2.3658E+01	1.8919E+01	1.9727E+01	1.9047E+01	**1.3439E+01**	1.7049E+01
	Best	5.6024E+02	**5.1987E+02**	5.3778E+02	5.4331E+02	5.3338E+02	5.4765E+02	5.4219E+02
	Rank	7	5	3	6	2	1	4
f_6	Ave	6.7714E+02	6.4724E+02	6.4625E+02	6.4591E+02	**6.4466E+02**	6.4994E+02	6.4936E+02
	Std	2.1889E+01	1.6427E+01	1.4609E+01	1.7418E+01	1.8144E+01	1.5923E+01	**1.4425E+01**
	Best	6.3055E+02	6.2341E+02	**6.1338E+02**	6.2035E+02	6.1464E+02	6.1950E+02	6.2688E+02
	Rank	7	4	3	2	1	6	5
f_7	Ave	1.0644E+03	8.5809E+02	8.7279E+02	8.8366E+02	**8.5724E+02**	8.6507E+02	8.8234E+02
	Std	1.4443E+02	**4.4999E+01**	5.8525E+01	6.3248E+01	4.9121E+01	5.8268E+01	6.1988E+01
	Best	8.3260E+02	7.7539E+02	7.9872E+02	7.8404E+02	**7.7102E+02**	7.7617E+02	7.9473E+02
	Rank	7	2	4	6	1	3	5
f_8	Ave	9.1465E+02	8.6852E+02	8.6887E+02	8.7256E+02	8.7151E+02	8.6929E+02	**8.6648E+02**
	Std	2.9096E+01	1.9874E+01	2.1774E+01	1.9157E+01	1.6824E+01	2.1134E+01	**1.6103E+01**
	Best	8.6317E+02	8.4280E+02	8.3831E+02	8.3294E+02	8.4116E+02	**8.2993E+02**	8.3578E+02
	Rank	7	2	3	6	5	4	1
f_9	Ave	4.4972E+03	2.4785E+03	2.5108E+03	2.3895E+03	**2.3389E+03**	2.8259E+03	2.6431E+03
	Std	1.4497E+03	6.9721E+02	1.0464E+03	7.0209E+02	**6.5554E+02**	1.4320E+03	9.1201E+02
	Best	2.2238E+03	1.3851E+03	1.0921E+03	1.1464E+03	1.3088E+03	**1.0728E+03**	1.3340E+03

	Rank	7	3	4	2	1	6	5
	Ave	2.9789E+03	**2.6010E+03**	2.6443E+03	2.6971E+03	2.6710E+03	2.6474E+03	2.7345E+03
f_{10}	Std	**2.1466E+02**	2.6233E+02	2.6124E+02	3.6212E+02	2.7108E+02	3.7529E+02	3.5876E+02
	Best	2.5534E+03	2.0145E+03	2.1802E+03	1.7909E+03	2.0767E+03	**1.6409E+03**	2.1983E+03
	Rank	7	1	2	5	4	3	6
	Ave	8.3627E+03	2.0527E+03	**1.8351E+03**	2.4128E+03	1.8762E+03	2.3441E+03	2.2022E+03
f_{11}	Std	1.0752E+04	1.9565E+03	**6.5789E+02**	1.8909E+03	1.0686E+03	1.2941E+03	1.3011E+03
	Best	1.5489E+03	1.1948E+03	1.1721E+03	1.2319E+03	**1.2115E+03**	1.2741E+03	1.2498E+03
	Rank	7	3	1	6	2	5	4
	Ave	8.2080E+08	2.5885E+07	4.9370E+07	4.2063E+07	**2.2016E+07**	4.6307E+07	4.8686E+07
f_{12}	Std	6.7686E+08	3.7168E+07	7.4182E+07	4.6549E+07	**3.0594E+07**	3.9490E+07	8.7459E+07
	Best	1.1454E+07	1.1942E+06	1.1629E+06	2.1204E+06	**8.9631E+05**	5.1177E+06	1.2305E+06
	Rank	7	2	6	3	1	4	5
	Ave	5.2660E+07	**4.7968E+04**	1.9944E+05	3.5911E+05	1.0004E+05	2.5392E+05	5.3140E+05
f_{13}	Std	1.0165E+08	**3.9608E+04**	4.1475E+05	6.0584E+05	1.5777E+05	3.4679E+05	1.8527E+06
	Best	2.1838E+04	4.9847E+03	3.3986E+03	**1.9060E+03**	7.4217E+03	5.3095E+03	4.6828E+03
	Rank	7	1	3	5	2	4	6
	Ave	1.3594E+06	8.1121E+03	8.3235E+03	9.8709E+03	**7.6682E+03**	9.8471E+03	1.0469E+04
f_{14}	Std	4.1693E+06	**7.5114E+03**	8.3607E+03	9.5344E+03	8.0287E+03	8.2608E+03	9.7261E+03
	Best	2.3773E+03	1.5216E+03	1.6288E+03	**1.4827E+03**	1.5055E+03	1.5900E+03	1.6349E+03
	Rank	7	2	3	5	1	4	6
	Ave	1.3721E+06	6.2922E+04	4.3062E+04	4.1696E+04	**2.8810E+04**	5.2001E+04	4.0911E+04
f_{15}	Std	3.6867E+06	8.9259E+04	3.5862E+04	4.8943E+04	**2.8772E+04**	6.5569E+04	4.3704E+04
	Best	8.5202E+03	3.1418E+03	**2.5549E+03**	2.8760E+03	3.3676E+03	2.7852E+03	3.2252E+03
	Rank	7	6	4	3	1	5	2
	Ave	2.3757E+03	2.0309E+03	2.0148E+03	2.1248E+03	**1.9745E+03**	2.0216E+03	2.0576E+03
f_{16}	Std	2.0877E+02	1.6807E+02	1.6743E+02	1.6570E+02	1.6461E+02	**1.6186E+02**	1.9429E+02
	Best	1.9254E+03	1.7893E+03	**1.6826E+03**	1.8153E+03	1.7587E+03	1.7538E+03	1.7025E+03
	Rank	7	4	2	6	1	3	5
	Ave	2.1432E+03	1.8896E+03	**1.8499E+03**	1.8926E+03	1.9080E+03	1.8890E+03	1.9261E+03
f_{17}	Std	1.9557E+02	8.7623E+01	**5.2694E+01**	9.2250E+01	9.7723E+01	9.1628E+01	9.9131E+01
	Best	1.8225E+03	1.7563E+03	1.7675E+03	1.7598E+03	**1.7521E+03**	1.7330E+03	1.7694E+03
	Rank	7	3	1	4	5	2	6
	Ave	1.4040E+08	4.0945E+05	1.1789E+05	9.1801E+05	**6.5132E+04**	4.7324E+05	3.4314E+05
f_{18}	Std	2.1836E+08	1.2964E+06	3.7270E+05	2.7067E+06	**6.2203E+04**	9.2143E+05	6.9500E+05
	Best	5.1202E+04	**3.7971E+03**	8.0108E+03	1.1846E+04	6.0044E+03	9.8495E+03	1.4085E+04
	Rank	7	4	2	6	1	5	3
	Ave	2.2152E+06	**9.2973E+04**	2.4192E+05	1.3200E+05	9.7480E+04	2.6435E+05	1.3503E+05
f_{19}	Std	3.1358E+06	**1.0286E+05**	8.4464E+05	3.9323E+05	1.4787E+05	6.0714E+05	2.5494E+05
	Best	2.9562E+04	6.5456E+03	3.7284E+03	2.2818E+03	**2.1329E+03**	2.2469E+03	3.6059E+03
	Rank	7	1	5	3	2	6	4
	Ave	2.3880E+03	**2.2224E+03**	2.2521E+03	2.2365E+03	2.2559E+03	2.2329E+03	2.2668E+03
f_{20}	Std	1.2195E+02	8.7267E+01	9.2257E+01	**7.4692E+01**	1.0284E+02	1.0508E+02	1.0015E+02
	Best	2.1192E+03	2.0917E+03	2.0621E+03	2.1012E+03	2.0655E+03	**2.0479E+03**	2.0586E+03
	Rank	7	1	4	3	5	2	6
	Ave	2.3863E+03	2.3545E+03	2.3463E+03	2.3650E+03	**2.3381E+03**	2.3547E+03	2.3549E+03
f_{21}	Std	5.5201E+01	4.2540E+01	5.1313E+01	**4.1699E+01**	5.8320E+01	4.4785E+01	4.4972E+01
	Best	2.2699E+03	2.2349E+03	**2.2087E+03**	2.2333E+03	2.1192E+03	2.2407E+03	2.2214E+03
	Rank	7	3	2	6	1	4	5
	Ave	3.3501E+03	2.5447E+03	2.7110E+03	2.7000E+03	**2.5443E+03**	2.6872E+03	2.7058E+03
f_{22}	Std	6.1609E+02	**1.3711E+02**	5.4218E+02	5.5826E+02	2.8885E+02	4.6951E+02	4.5760E+02
	Best	2.5424E+03	2.3280E+03	**2.2594E+03**	2.3296E+03	2.2948E+03	2.3161E+03	2.3971E+03

	Rank	7	2	6	4	1	3	5
f_{23}	Ave	2.7115E+03	2.6654E+03	**2.6627E+03**	2.6709E+03	2.6629E+03	2.6637E+03	2.6661E+03
	Std	2.6397E+01	1.8255E+01	1.5787E+01	**1.3996E+01**	1.8177E+01	1.9640E+01	1.5664E+01
	Best	2.6600E+03	**2.6266E+03**	2.6274E+03	2.6488E+03	2.6370E+03	2.6268E+03	2.6368E+03
	Rank	7	4	1	6	2	3	5
f_{24}	Ave	2.8526E+03	2.7919E+03	2.7917E+03	2.7928E+03	**2.7841E+03**	2.7972E+03	2.7883E+03
	Std	3.9366E+01	1.9027E+01	2.2807E+01	3.7523E+01	4.2896E+01	**1.7824E+01**	5.2217E+01
	Best	2.7780E+03	2.7545E+03	2.6961E+03	2.6768E+03	2.6142E+03	2.7652E+03	**2.6051E+03**
	Rank	7	4	3	5	1	6	2
f_{25}	Ave	3.6924E+03	3.0943E+03	3.1057E+03	3.1683E+03	**3.0839E+03**	3.1557E+03	3.1584E+03
	Std	5.2753E+02	1.5471E+02	1.4369E+02	**1.3707E+02**	1.4031E+02	1.7855E+02	2.0545E+02
	Best	3.0269E+03	2.9535E+03	**2.9422E+03**	2.9711E+03	2.9604E+03	2.9717E+03	2.9468E+03
	Rank	7	2	3	6	1	4	5
f_{26}	Ave	4.0366E+03	3.6143E+03	3.6728E+03	3.7117E+03	**3.4206E+03**	3.6311E+03	3.6159E+03
	Std	6.0893E+02	5.2751E+02	5.7499E+02	5.4367E+02	**3.3267E+02**	5.3344E+02	4.8124E+02
	Best	3.1752E+03	**2.9953E+03**	3.0247E+03	3.0910E+03	3.0416E+03	3.0639E+03	3.1286E+03
	Rank	7	2	5	6	1	4	3
f_{27}	Ave	3.1636E+03	3.1263E+03	3.1231E+03	**3.1218E+03**	3.1271E+03	3.1326E+03	3.1245E+03
	Std	3.9485E+01	2.8888E+01	2.8006E+01	2.7017E+01	3.2869E+01	3.7793E+01	**2.5699E+01**
	Best	3.1091E+03	3.1027E+03	3.0984E+03	3.1024E+03	3.1012E+03	**3.0969E+03**	3.1011E+03
	Rank	7	4	2	1	5	6	3
f_{28}	Ave	3.6971E+03	3.4549E+03	3.4704E+03	3.5177E+03	**3.4503E+03**	3.5034E+03	3.4556E+03
	Std	1.6080E+02	1.3913E+02	1.3243E+02	1.6439E+02	1.4902E+02	**1.1609E+02**	1.4779E+02
	Best	3.4116E+03	3.2698E+03	3.2419E+03	**3.2234E+03**	3.2298E+03	3.2847E+03	3.2240E+03
	Rank	7	2	4	6	1	5	3
f_{29}	Ave	3.6246E+03	3.3976E+03	**3.3582E+03**	3.4442E+03	3.3681E+03	3.4104E+03	3.4027E+03
	Std	1.7003E+02	1.2995E+02	**8.8909E+01**	1.4038E+02	9.6805E+01	1.2120E+02	1.1673E+02
	Best	3.3635E+03	3.1931E+03	**3.1776E+03**	3.2166E+03	3.2101E+03	3.2090E+03	3.2058E+03
	Rank	7	3	1	6	2	5	4
f_{30}	Ave	6.5849E+06	4.7172E+06	**3.5766E+06**	6.0177E+06	4.3510E+06	5.4049E+06	4.6667E+06
	Std	9.7970E+06	5.0039E+06	3.1980E+06	6.3849E+06	8.2775E+06	5.3262E+06	**3.0312E+06**
	Best	8.8586E+05	5.9917E+05	**5.1145E+04**	3.0707E+05	2.0599E+05	3.0977E+05	1.0367E+05
	Rank	7	4	1	6	2	5	3
Friedman		7	2.8	2.87	4.9	2	4.17	4.27
Rank		7	2	3	6	1	4	5

B. HSSFOA solves the ELD problem of Case 1

In this section and the next, the effectiveness and robustness of the proposed HSSFOA algorithm are thoroughly evaluated through comparative experiments on two real-world economic load dispatch (ELD) problems with different system scales. Across both experiments, the SISFOA algorithm-which demonstrated competitive performance in earlier tests-is adopted as a baseline reference. Additionally, several well-established metaheuristic algorithms are included for the benchmarking purposes, namely the original Superb Fairy-wren Optimization Algorithm (SFOA), Arithmetic Optimization Algorithm (AOA) [18], Whale Optimization Algorithm (WOA) [15], Bermuda Triangle Optimizer (BTO) [19] and Divine Religions Algorithm (DRA) [20]. These algorithms are selected due to their strong track records in solving complex, nonlinear, and constrained optimization problems, making them suitable candidates for a fair and rigorous comparison.

To enhance the realism and difficulty of the problem, valve-point loading effects are incorporated into the system model. This inclusion introduces ripples in the fuel cost functions, making the optimization landscape more intricate and challenging. Such a configuration serves to thoroughly test the adaptability and convergence capabilities of each algorithm under more practical and nonlinear conditions. The specific parameter settings for all compared algorithms are summarized in Table III.

Since the valve-point effects are considered in this study, the mathematical formulation of the economic load dispatch (ELD) problem is represented by Eq. (17).

$$MinF_i = \sum_{i=1}^{n} (\alpha_i + \beta_i P + \gamma_i P_i^2 + |e_i \times sin(f_i(P_i^{min} - P_i))|) \quad (17)$$

where, F_i denotes the total fuel cost, and P_i represents the power output of the i-th generator. The variable n denotes the total number of generating units. The constants α_i, β_i, and γ_i are the fuel cost coefficients specific to the i-th generator. The parameters e_i and f_i are coefficients associated with the valve-point effect of the i-th generator, while P_i^{min} represents the minimum allowable power output of the i-th unit.

To demonstrate the practical applicability of the proposed HSSFOA, a classical 6-unit economic load dispatch (ELD) problem is considered as the first real-world benchmark. The objective of this problem is to allocate power generation among six thermal units to meet a total load demand of 1263 MW while minimizing the total generation cost. The problem incorporates realistic operational constraints, including generator capacity limits and transmission line losses, making it a suitable test case for validating both feasibility and optimization performance. Each algorithm is executed independently over multiple runs and the results are evaluated based on minimum cost and convergence behavior.

This 6-unit ELD case serves as a foundational scenario to verify the consistency and reliability of HSSFOA in handling constrained, nonlinear optimization tasks in power systems. In the 6-unit ELD experiment, all algorithms are employed to solve the economic load dispatch problem of thermal power units. The basic experimental settings are as follows. The maximum number of iterations is set to 1000, the population size is 20 and the problem dimension is 6. Each algorithm is independently executed 20 times to calculate the average performance. The fuel cost coefficients and generation limits of the units are listed in Table IV. The convergence curves of the algorithms are illustrated in Fig. 5, and the corresponding numerical results are summarized in Table V. A comparison of the total fuel costs obtained by different algorithms is provided in Table VI. Fig. 6 shows the histogram of the total fuel cost of 6 units.

TABLE III. PARAMETER SETTINGS OF EACH ALGORITHM

Algorithm	Main parameters setting
SFOA	*C*=0.8; *T*=0.5;
SISFOA	*C*=0.8; *T*=0.5;
AOA[18]	MOAmax=1; MOAmax=0.2; Alpha=5; Mu=0.499
WOA[15]	*b*=1;
BTO[19]	POFmax =log(1.510000); POFmin =log(500000); g=6.67e-11;
DRA[20]	BPSP=0.5; MP=0.5; PP=0.9; RP=0.2;

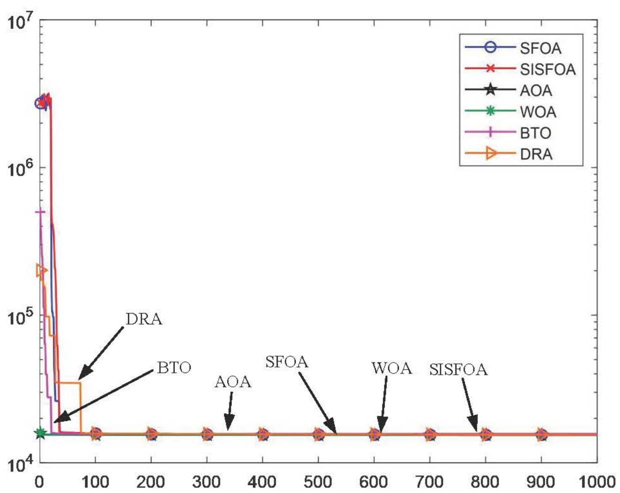

Fig. 5 Convergence diagram of comparative experiment.

TABLE IV. THE FUEL COST COEFFICIENTS AND POWER GENERATION LIMITS OF THE 6 GENERATING UNITS

Unit	α_i	β_i	γ_i	P_{max}	P_{min}
1	240	7.0	0.0070	500	100
2	200	10.0	0.0095	200	50
3	220	8.5	0.0090	300	80
4	200	11.0	0.0090	150	50
5	220	10.5	0.0080	200	50
6	190	12.0	0.0075	120	50

TABLE V. EXPERIMENTAL RESULTS CONTRASTING

Unit	SFOA	SISFOA	AOA[18]	WOA[15]	BTO[19]	DRA[20]
P_1	500	500	481.34	446.13	500	382.15
P_2	168.92	200	175.57	192.67	165.35	174.52
P_3	292.48	252.46	267.67	217.11	300	300
P_4	138.24	101.06	150	144.70	150	150
P_5	77.68	152.39	140	160.89	50	174.52
P_6	92.16	63.89	55.29	107.55	120	96.96
P_L	6.40	6.55	6.17	6.05	6.77	6.30
P_D	1269.49	1269.79	1269.86	1269.05	1285.35	1278.15

TABLE VI. COMPARISON OF EXPERIMENTAL RESULTS

Method	Generation cost ($)
SFOA	15430.85
SISFOA	15395.39
AOA[18]	15396.08
WOA[15]	15407.42
BTO[19]	15684.19
DRA[20]	15521.46

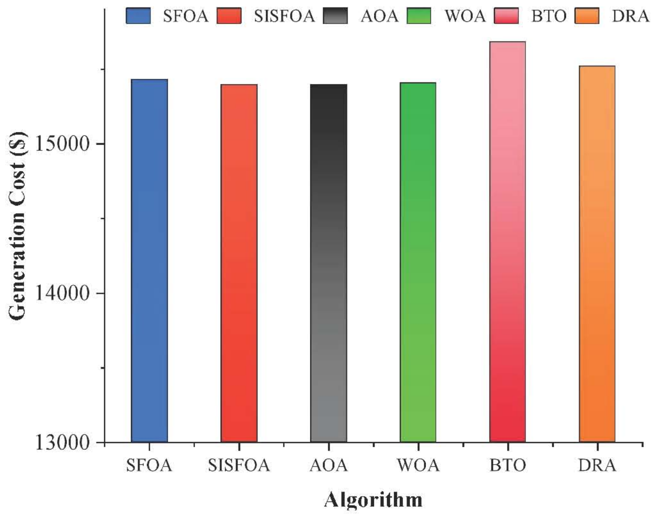

Fig. 6 The histogram of the total fuel cost of 6 units.

According to the data presented in Tables V-VI, the SISFOA algorithm achieves the lowest total fuel cost of $15,395.39, representing an improvement of approximately 0.22% over the original SFOA. This demonstrates the effectiveness of the improved hybrid strategy in enhancing the solution quality. SISFOA demonstrates a favorable trade-off between cost minimization and power loss management, confirming its robustness and effectiveness in solving constrained economic load dispatch problems.

C. HSSFOA solves the ELD problem of Case 2

To further evaluate the scalability and effectiveness of the proposed HSSFOA in solving large-scale and highly constrained optimization problems, a more complex 20-unit economic load dispatch (ELD) case is investigated. All algorithms are applied to the economic load dispatch (ELD) problem involving 20 thermal generating units with a total power demand of 2500 MW. The basic experimental settings for the 20-unit ELD case are as follows. The maximum number of iterations is set to 1000, the population size is fixed at 20 and the problem dimension is 20. Each algorithm is independently executed 20 times to evaluate average performance and statistical reliability. Table VII presents the fuel cost coefficients and power generation limits of the generating units. The experimental convergence curves are shown in Fig. 7, and the corresponding numerical results and the total fuel cost are summarized in Table VIII. The comparison of total fuel costs is presented in Table IX. Fig. 8 shows the histogram of the total fuel cost of 20 units. Based on the results shown in Tables VIII, it is evident that the SISFOA achieves the lowest total fuel cost, amounting to \$62,039.19. Compared to the original algorithm, this represents a cost reduction of approximately 0.08%. Although the percentage improvement may appear modest, such reductions are significant in large-scale power systems, where even marginal improvements can result in substantial economic savings over extended periods of operation. This demonstrates the superior performance and enhanced optimization capability of SISFOA in addressing complex economic load dispatch problems with valve-point effects.

TABLE VII. THE FUEL COST COEFFICIENTS AND POWER GENERATION LIMITS OF THE 20 GENERATING UNITS

Unit	α_i	β_i	γ_i	P_{min}	P_{max}
1	1000	18.19	0.00068	150	600
2	970	19.26	0.00071	50	200
3	600	19.80	0.00650	50	200
4	700	19.10	0.00500	50	200
5	420	18.10	0.00738	50	160
6	360	19.26	0.00612	20	100
7	490	17.14	0.00790	25	125
8	660	18.92	0.00813	50	150
9	765	18.27	0.00522	50	200
10	770	18.92	0.00573	30	150
11	800	16.69	0.00480	100	300
12	970	16.76	0.00310	150	500
13	900	17.36	0.00850	40	160
14	700	18.70	0.00511	20	130
15	450	18.70	0.00398	25	185
16	370	14.26	0.07120	20	80
17	480	19.14	0.00890	30	85
18	680	18.92	0.00713	30	120
19	700	18.47	0.00622	40	120
20	850	19.79	0.00773	30	100

TABLE VIII. EXPERIMENTAL RESULTS CONTRASTING

Unit	SFOA	SISFOA	AOA[18]	WOA[15]	BTO[19]	DRA[20]
P_1	235.56	292.78	600	249.58	548.37	381.91
P_2	160.11	157.67	95.62	139.21	148.95	127.30
P_3	103.26	92.91	95.62	73.76	132.96	127.30
P_4	184.68	176.32	55.44	92.81	60.44	127.30
P_5	52.39	147.42	160	50.91	128.54	127.30
P_6	94.93	82.36	20	97.41	70.12	50.92
P_7	68.03	98.73	28.45	34.05	57.95	63.65
P_8	74.97	97.28	50	123.69	131.88	127.30
P_9	200	99.56	50	189.85	146.28	127.30
P_{10}	115.67	120.38	51.63	88.87	124.00	76.38
P_{11}	275.28	115.58	129.17	191.56	199.64	254.60
P_{12}	327.68	390.21	500	408.86	246.48	381.91
P_{13}	108.94	56.90	160	141.34	47.88	101.84
P_{14}	94.26	112.82	130	101.64	74.89	50.92
P_{15}	87.94	185	74.27	163.63	145.64	63.65
P_{16}	52.85	70.00	20	69.80	24.78	50.92
P_{17}	63.22	48.18	30	68.65	35.27	76.38
P_{18}	83.20	36.06	120	98.56	110.06	76.38
P_{19}	102.96	89.54	120	87.75	87.19	101.84
P_{20}	82.06	94.19	100	94.91	66.22	76.38
P_L	67.93	63.89	77.63	66.83	63.95	68.20
P_D	2567.98	2563.89	2590.19	2566.83	2587.54	2571.51
Generation Cost (\$)	62093.20	62039.19	62326.45	62104.71	62386.35	62092.04

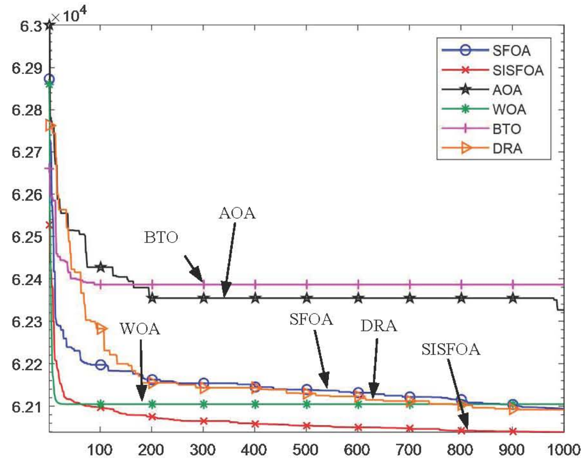

Fig. 7 Convergence diagram of comparative experiment.

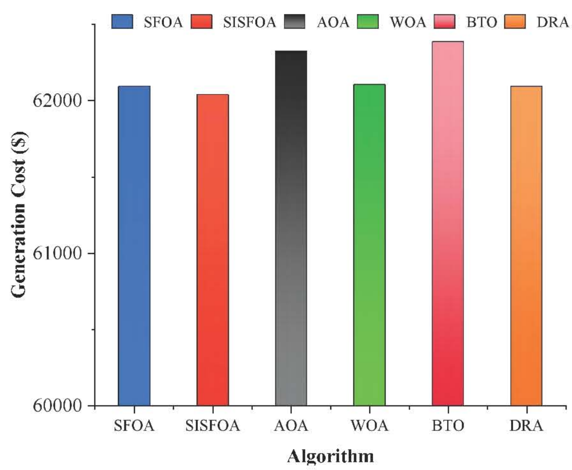

Fig. 8 The histogram of the total fuel cost of 20 units

V. CONCLUSION

The Hybrid Spiral Superb Fairy-wren Optimization Algorithm (HSSFOA) proposed in this study effectively enhances the collaborative capability between global exploration and local development by integrating the random jump mechanism of the Harris Hawks Optimization (HHO) algorithm with the spiral search strategy of the Whale Optimization Algorithm (WOA) into the three-phase behavior model of the Superb Fairy-wren Optimization Algorithm (SFOA). This hybrid framework not only preserves the structural diversity and dynamic adjustment capabilities of the original SFOA but also introduces a search mechanism with more pronounced jumping and non-linear characteristics. This significantly improves the algorithm's ability to escape local optima in complex high-dimensional search spaces and accelerates the overall convergence speed.

Furthermore, to explore the potential of the spiral search strategy in influencing the diversity of search paths and local convergence ability, this study designs and introduces five novel spiral update mechanisms: Sine Spiral, Phase-modulated Log Spiral, Hyperbolic Sine Spiral, Hyperbolic Cosine Spiral, and Damped Spiral. These spirals adjust the nonlinear amplitude and frequency of direction changes in individual search trajectories, allowing the algorithm to dynamically adapt to the local characteristics and multi-modal structures of complex objective functions at different stages, thereby enhancing its jumping diversity and development stability.

In order to verify the effectiveness of the improved algorithm, we use the CEC-2017 test function to test and verify it. The experimental results show that the improved HSSFOA and its variants are superior to the original SFOA on most test functions, and are more excellent in convergence speed and accuracy of the solutions. Among all the proposed variants, the SISFOA exhibited the most outstanding performance. Therefore, SISFOA was selected for further empirical validation in practical engineering applications through two case studies of the ELD problems with different scales and complexity. In a 6-unit generator set with a total demand of 1263 MW, we conducted a test. The improved SISFOA performs well in minimizing the total fuel cost while satisfying all operational constraints, and is superior to other algorithms in terms of convergence stability and solution quality.

The SISFOA achieves the lowest total fuel cost in all test algorithms again under a total demand of 2500 MW for 20 units. The two results prove that the improved algorithm performs well in different scale and complexity problems. It not only continues to outperform baseline and comparison algorithms in terms of cost optimization, but also shows stable convergence characteristics and strong adaptability to actual constraints. The algorithm can still maintain a high level of solution quality and computational stability under strict problem setting, which further highlights its robustness, scalability and practicability in power system operation and other fields that require complex optimization strategies.

REFERENCES

[1] J. Emmanuel, I. Isewon, and J. Oyelade. "An optimized deep-forest algorithm using a modified differential evolution optimization algorithm: A case of host-pathogen protein-protein interaction prediction," *Computational and Structural Biotechnology Journal*, vol. 27, pp. 595-611, 2025.

[2] A. Pradhan, A. Das, and S. K. Bisoy. "Modified parallel PSO algorithm in cloud computing for performance improvement," *Cluster Computing*, vol. 28, no. 2, pp. 131, 2025.

[3] Y. Wang, X. Yu, and W. Zhang. "An improved reinforcement learning-based differential evolution algorithm for combined economic and emission dispatch problems," *Engineering Applications of Artificial Intelligence*, vol. 140, pp. 109709, 2025.

[4] P. Lahande, P. Kaveri, and H. Singh. "EM-ACO-ARM: An enhanced multiple ant colony optimization algorithm for adaptive resource management in cloud environment," *Procedia Computer Science*, vol. 252, pp. 796-805, 2025.

[5] R. Fang, T. Zhou, and B. Yu. "Dung beetle optimization algorithm based on improved multi-strategy fusion," *Electronics*, vol. 14, no. 1, pp. 197, 2025.

[6] Y. Wang, X. Yu, and W. Zhang. "An improved reinforcement learning-based differential evolution algorithm for combined economic and emission dispatch problems," *Engineering Applications of Artificial Intelligence*, vol. 140, pp. 109709, 2025.

[7] Y. Xu, R. Zhong, and Y. Cao. "Symbiotic mechanism-based honey badger algorithm for continuous optimization," *Cluster Computing*, vol. 28, no. 2, pp. 133, 2025.

[8] L. Chaib, M. Tadj, and A. Choucha. "Improved crayfish optimization algorithm for parameters estimation of photovoltaic models," *Energy Conversion and Management*, vol. 313, pp. 118627, 2024.

[9] H. Jia, X. Zhou, and J. Zhang, "Modified crayfish optimization algorithm for solving multiple engineering application problems," *Artificial Intelligence Review*, vol. 57, no. 5, pp. 127, 2024.

[10] Y. Chun, X. Hua, and C. Qi. "Improved marine predators algorithm for engineering design optimization problems," *Scientific Reports*, vol. 14, no. 1, pp. 13000, 2024.

[11] L. Qian, M. Khishe, and Y. Huang. "SEB-ChOA: An improved chimp optimization algorithm using spiral exploitation behavior," *Neural Computing and Applications*, vol. 36, no. 9, pp. 4763-4786, 2024.

[12] T. Huang, F. Huang, and Z. Qin. "An improved polar lights optimization algorithm for global optimization and engineering applications," *Scientific Reports*, vol. 15, no. 1, pp. 11581, 2025.

[13] H. Jia, X. Zhou, and J. Zhang. "Superb fairy-wren optimization algorithm: A novel metaheuristic algorithm for solving feature selection problems," *Cluster Computing*, vol. 28, no. 4, pp. 246, 2025.

[14] A. A. Heidari, S. Mirjalili, and H. Faris. "Harris hawks optimization: algorithm and applications," *Future Generation Computer Systems*, vol. 97, pp. 849-872, 2019.

[15] S. Mirjalili and A. Lewis. "The whale optimization algorithm," *Advances in Engineering Software*, vol. 95, pp. 51-67, 2016.

[16] M. Nemati, Y. Zandi, and A. S. Agdas. "Application of a novel metaheuristic algorithm inspired by stadium spectators in global optimization problems," *Scientific Reports*, vol. 14, no. 1, pp. 3078, 2024.

[17] K. E. Fahim, L. C. D. Silva, and V. Andiappan. "A novel hybrid algorithm for solving economic load dispatch in power systems," *International Journal of Energy Research*, vol. 1, pp. 8420107, 2024.

[18] L. Abualigah, A. Diabat, and S. Mirjalili. "The arithmetic optimization algorithm," *Computer Methods in Applied Mechanics and Engineering*, vol. 376, pp. 113609, 2021.

[19] H. A. Shehadeh. "Bermuda triangle optimizer (BTO): A novel metaheuristic method for global optimization," *International Journal of Advances in Soft Computing and its Applications*, vol. 17, no. 2, pp. 1-18, 2025.

[20] A. T. Mozhdehi, N. Khodadadi, and M. Aboutalebi. "Divine religions algorithm: A novel social-inspired metaheuristic algorithm for engineering and continuous optimization problems," *Cluster Computing*, vol. 28, no. 4, pp. 253, 2025.